Role of nitrogen in AlNxMn3: A density functional theory study

D. F. Shao, W. J. Lu, J. C. Lin, P. Tong, H. B. Jian et al.

Citation: J. Appl. Phys. **113**, 023905 (2013); doi: 10.1063/1.4774314
View online: http://dx.doi.org/10.1063/1.4774314
View Table of Contents: http://jap.aip.org/resource/1/JAPIAU/v113/i2
Published by the AIP Publishing LLC.

JOURNAL OF APPLIED PHYSICS **113**, 023905 (2013)

Role of nitrogen in AlN_xMn_3: A density functional theory study

D. F. Shao,[1] W. J. Lu,[1,a)] J. C. Lin,[1] P. Tong,[1] H. B. Jian,[1] and Y. P. Sun[1,2,b)]
[1]*Key Laboratory of Materials Physics, Institute of Solid State Physics, Chinese Academy of Sciences, Hefei 230031, People's Republic of China*
[2]*High Magnetic Field Laboratory, Chinese Academy of Sciences, Hefei 230031, People's Republic of China*

(Received 26 September 2012; accepted 18 December 2012; published online 10 January 2013)

Recently, we successfully synthesized the nitrogen-deficient manganese antiperovskites AlN_xMn_3 with the very high ferromagnetic Curie temperatures T_C up to 818 K [Lin *et al.*, Appl. Phys. Lett. **98**, 092507 (2011)]. In order to figure out the role of nitrogen for the magnetism, in the present work, we performed a theoretical investigation on AlN_xMn_3 through the first-principles calculation based on density functional theory. The results show that AlN_xMn_3 have the ferromagnetic ground states, and the total magnetic moments in a cell are enhanced with decreasing the nitrogen concentration. Based on the calculations of band structure and density of states, we showed the influence of nitrogen concentration on magnetism for AlN_xMn_3: The decreasing of nitrogen concentration from ideal $AlNMn_3$ moves the spin-down bands towards the high energy remarkably, which enhances the exchange splitting energy ΔE_{ex}; on the other hand, nitrogen deficiency reduces the Mn-N hybridizations, which makes the 3*d* electrons of Mn tend to occupy the spin-up states. The nitrogen deficiency reduces the Mn-N hybridization, which narrows Mn-*d* bands and enhances the spin polarization. Furthermore, we estimated T_C of AlN_xMn_3, and found the calculated T_C can be scaled by spin fluctuation temperature T_{SF}, suggesting AlN_xMn_3 belong to the spin fluctuation system. © *2013 American Institute of Physics*. [http://dx.doi.org/10.1063/1.4774314]

I. INTRODUCTION

Antiperovskites compounds AXM_3 (A, main group elements; X, carbon, boron, or nitrogen; M, transition metal) were extensively studied in recent years due to the abundant physical properties such as superconductivities,[1,2] giant magnetoresistance (MR),[3,4] large negative magnetocaloric effect (MCE),[5,6] giant negative thermal expansion,[7,8] magnetostriction,[9] and nearly zero temperature coefficient of resistivity.[10,11] The common technique for producing AXM_3 sample is solid-state synthesis from the parent materials. The preparation must perform in oxygen-free environments, sometimes need high pressure, for example, the synthesis of $CdCNi_3$.[2] However, even in these strict conditions, it is still hard to obtain the stoichiometric compounds. Due to the small atomic mass of C and N, it is hard to detect the concentration of them accurately. Therefore, researchers often labeled their sample with a nominal stoichiometry obtained by the ratio of parent materials, or denoted with a nominal stoichiometry as $AX_{1\pm\delta}M_3$ with approximate value of δ.[12,13,17] The properties of AXM_3 are very sensitive to the X stoichiometry,[14,15] thus an inaccurate stoichiometry easily leads to misinterpretation.[16] Therefore, precise detections must be developed and applied to the compounds; on the other hand, researchers need to figure out the role of X for the properties of AXM_3.

Recently, we successfully synthesized the manganese nitride antiperovskites AlN_xMn_3.[17] AlN_xMn_3 show a soft ferromagnetic (FM) property with the FM Curie temperatures T_C up to 818 K, much higher than the theoretically estimated value (250 K)[18] and T_C of Mn_4N (740 K).[19,20] As the problem we mentioned before, we labeled the stoichiometry with $x = 1.0$, 1.1, and 1.2 using the ratio of parent materials. But the lattice variety of them is only about 0.17%. Thus, we consider the real concentration of them must be very close to each other. Even the nominal N-concentrations are larger than 1, the real concentration should be equal to or less than 1, which means the samples with $x = 1.2$ may be nitrogen deficient.

In order to figure out the role of nitrogen for the magnetism, in the present work we performed a theoretical investigation on AlN_xMn_3 ($x = 0 \sim 1$) through the first-principles calculation based on density functional theory (DFT). AlN_xMn_3 show FM ground states, and the nitrogen deficiency enhances the total magnetic moment. Based on the calculated band structure and density of state (DOS), we find the decreasing of nitrogen concentration from ideal $AlNMn_3$ moves the spin-down bands towards the high energy, which enhances the exchange splitting energy ΔE_{ex}; on the other hand, the nitrogen deficiency reduces the Mn-N hybridizations, which makes the 3*d* electrons of Mn tend to occupy the spin-up states. It can be concluded that the nitrogen deficiency reduces the Mn-N hybridization and narrows Mn-*d* bands, and thus enhances the spin polarization. Furthermore, we estimated T_C for AlN_xMn_3. For the ideal $AlN_{0.917}Mn_3$, the estimated T_C is 835 K, which can be reasonably compared with the experimental value. The magnetic properties in the nitrogen-deficient AlN_xMn_3 can be described by a spin fluctuation system. By comparing the calculated T_C with experimental values, we evaluated the real stoichiometry of our previously synthesized AlN_xMn_3.

a)Electronic mail: wjlu@issp.ac.cn.
b)Electronic mail: ypsun@issp.ac.cn.

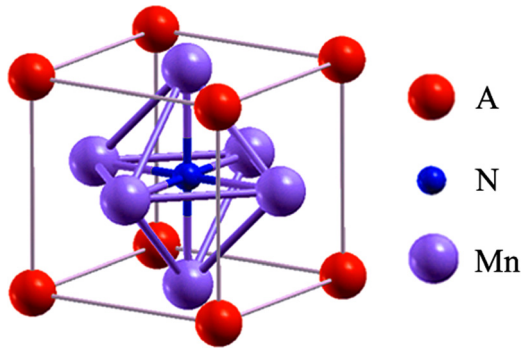

FIG. 1. The schematic structure of manganese nitride antiperovskite $ANMn_3$.

II. COMPUTIONAL DETAILS

The calculations were performed by pseudopotential plane-wave method, formalism implemented in the ABINIT code.[21–23] The exchange-correlation functions are treated using the generalized gradient approximation (GGA) according to the Perdew-Burke-Ernzerhof[24] parametrization. The norm-conserving pseudopotentials of Hartwigsen-Goedecker-Hutter (HGH) form[25] were used. Electronic wave functions are expanded with plane waves up to a high energy cutoff (E_{cut}) of 100 Ha. Brillouin zone sampling is performed on a Monkhorst-Pack (MP) mesh[26] of $12 \times 12 \times 12$. The self-consistent field (SCF) calculations were considered to be converged when the total energy of the system was stable within 10^{-6} eV per cell. Nonmagnetic (NM), FM, and antiferromagnetic (AFM) states were tested in the study.

III. RESULTS AND DISCUSSION

The structures of the manganese nitride antiperovskites AlN_xMn_3 ($x = 0 \sim 1$) were fully optimized for different magnetic configurations (Fig. 1). The SCF calculations show that the FM ground states have the lowest total energy. The optimized lattice parameters and magnetic moments in a formula unit are shown in Fig. 2. For $AlNMn_3$, the lattice parameter is 3.793 Å, which is close to the lattice parameter calculated by Ouyang *et al.*,[18] a little bit underestimated compared with the experimental results[17] (less than 2%).

The lattice parameters of AlN_xMn_3 decrease with decreasing the nitrogen concentration, and the magnetic moments vary with an opposite trend. The calculated total magnetic moment of $AlNMn_3$, the compound without nitrogen deficiency, is the minimum value of $3.09\mu_B$/f.u., which is close to the previous theoretically estimated value.[18] The maximum total magnetic moment is obtained in the hypothetic nitrogen-free compound $AlMn_3$ with a value of $6.33\mu_B$/f.u.. The role of nitrogen for magnetism will be discussed later.

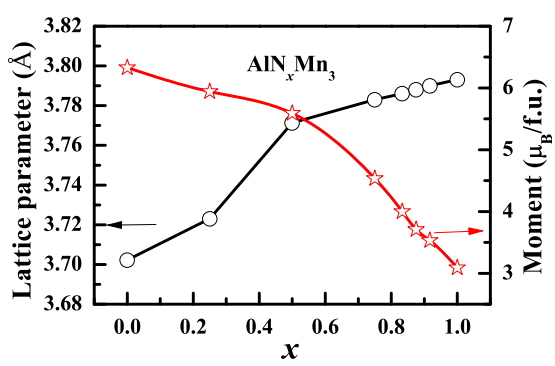

FIG. 2. The calculated lattice parameters and magnetic moments in a formula unit of AlN_xMn_3.

We calculated the electronic band structure of $AlNMn_3$ along the high symmetry directions in the Brillouin zone. The total and site-projected l-decomposed DOS of $AlNMn_3$ were also investigated. Here, we show the band structure and DOS of $AlNMn_3$ with NM state in Fig. 3. Bands from −8 eV to −5 eV are mainly from the N-2*p* and Mn-3*d* states with strong hybridizations characteristic. From −4 eV to 2 eV, there are hybridizations between N-2*p* and Mn-3*d* states, and the Mn-3*d* states contribute predominately to the bands, which suggest the itinerant nature of Mn-3*d* electrons.[18] There is a peak of DOS figure, which makes the DOS at Fermi level $N(E_F)$ higher than 8 states/eV. Such a high $N(E_F)$ can lead to magnetic instability.

In order to clarify the role of nitrogen for magnetism, we calculated the total and site-projected l-decomposed DOS of AlN_xMn_3 with the FM ground states. The DOS of AlN_xMn_3 shows similar shape (Fig. 4). The exchange splitting energy ΔE_{ex} between the spin-up and spin-down bands is estimated from the DOS figures and listed in Table I. Similar to the total magnetic moment, ΔE_{ex} is enhanced by nitrogen deficiency. The trends can be understood through the rigid band model: The loss of nitrogen reduces the electrons in the system, which makes the Fermi level low. The decreasing of Fermi energy can be seen as the states move toward the high energy side. From Fig. 4, it can be seen that the loss of nitrogen does not move the spin-up state effectively, but makes the spin-down states move to high energy levels remarkably. Therefore, the nitrogen deficiency enhances the exchange splitting.

We compared the electronic properties of the ideal $AlNMn_3$ and the nitrogen deficient $AlN_{0.5}Mn_3$ following Sieberer *et al.*[16] The electronic structure of $AlN_{0.5}Mn_3$ was calculated using a doubled unit cell, $Al_2N_1Mn_6$. Fig. 5 show the projected DOS for FM AlN_xMn_3 with $x = 0.5$ and $x = 1$. In the supercell $Al_2N_1Mn_6$, the six Mn atoms are divided into

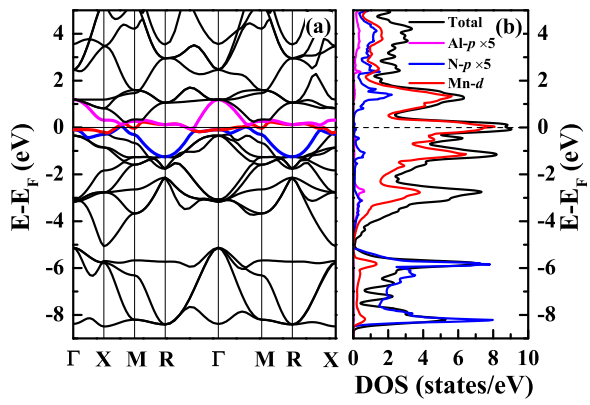

FIG. 3. (a) The band structure of $AlNMn_3$ with NM state. The colored lines denote the bands cross the Fermi level. (b) The density of states of $AlNMn_3$ with NM state.

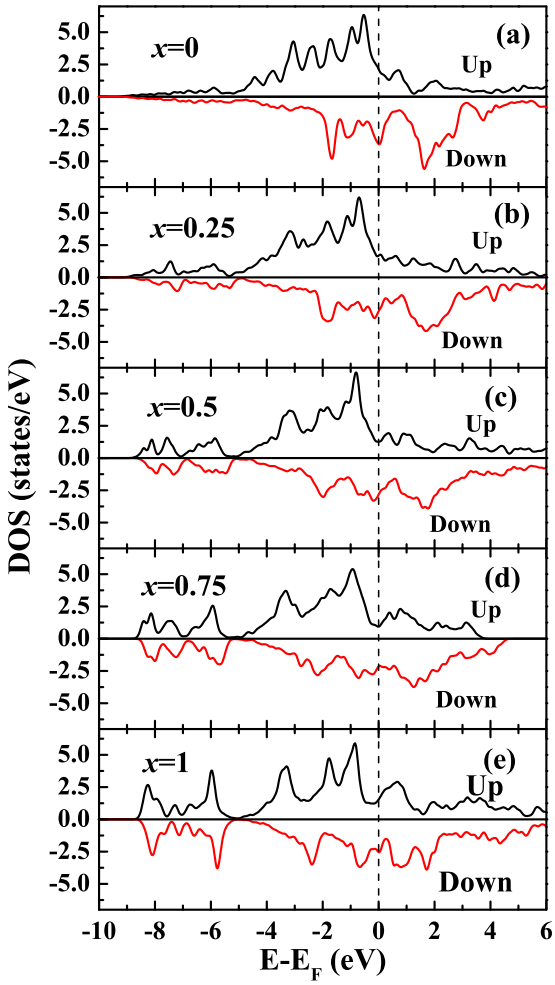

FIG. 4. The density of states for AlN_xMn_3 with FM states for (a) $x=0$, (b) $x=0.25$, (c) $x=0.5$, (d) $x=0.75$, and (e) $x=1$.

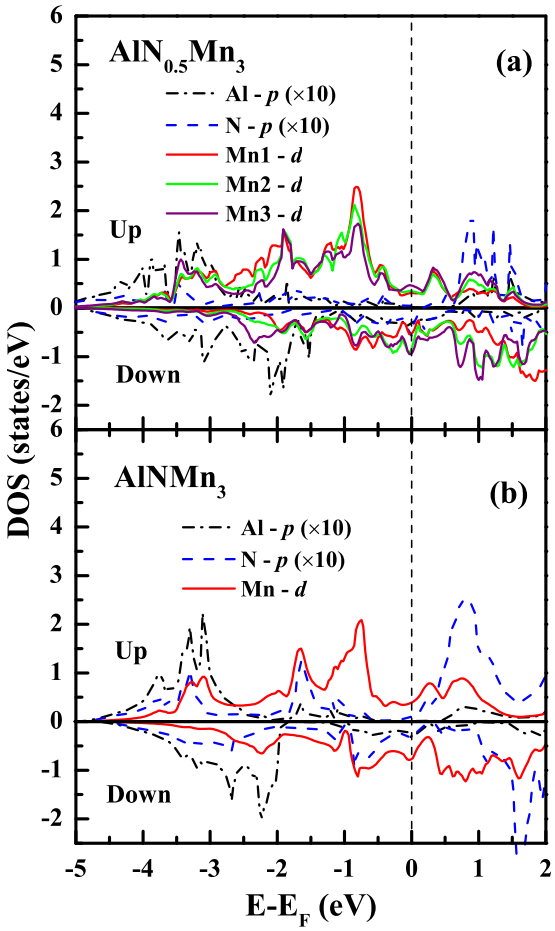

FIG. 5. The projected DOS for AlN_xMn_3 with FM states for (a) $x=0.5$ and (b) $x=1$.

three types: Mn1 denotes the Mn atoms without nitrogen neighbor, Mn2 denotes the Mn atoms with only one neighboring nitrogen, and Mn3 denotes the Mn atoms with two neighboring nitrogen.

The difference of the three types of Mn atoms is the strength of Mn-N hybridization. The lower the number of neighboring nitrogen, the weaker is the Mn-N hybridization. From Fig. 5(a), it can be seen that the weaker Mn-N hybridization leads to higher DOS of spin-up electrons and lower DOS of spin-down electrons. It suggests that for a weak Mn-N hybridization, the $3d$ electrons of Mn tend to occupy the spin-up states.

Different nitrogen vacancy arrangements may affect the electronic structure and magnetic property. Therefore, we compare the electronic structures of $AlN_{0.75}Mn_3$ with 3 different nitrogen vacancy arrangements. The calculation is using a $2\times2\times2$ supercell ($Al_8N_6Mn_24$), the distances between the nearest nitrogen vacancy is a (vacancies locate at (0.5, 0.5, 0.5) and (0.5, 0.5, 1.5)), $\sqrt{2}a$ (vacancies locate at (0.5, 0.5, 0.5) and (0.5, 1.5, 1.5)), and $\sqrt{3}a$ (vacancies locate at (0.5, 0.5, 0.5) and (1.5, 1.5, 1.5)), respectively. The magnetic moments and $N(E_F)$ for nitrogen vacancy arrangements

TABLE I. Calculated parameters of AlN_xMn_3: exchange splitting energy ΔE_{ex}, density of states at Fermi level for each Mn atom $N^{\uparrow}_{Mn}(E_F)$ and $N^{\downarrow}_{Mn}(E_F)$, magnetic moment per a Mn atom m, exchange integer I, Stoner temperature T_S, spin fluctuation temperature T_{SF}, Curie temperature T_C, and T_C/T_S ratios.

	ΔE_{ex} (eV)	$N^{\uparrow}_{Mn}(E_F)$ (states/eV/Mn)	$N^{\downarrow}_{Mn}(E_F)$ (states/eV/Mn)	m (μ_B/Mn)	I (eV)	T_S (K)	T_{SF} (K)	T_C (K)	T_C/T_S
$x=0$	1.73	0.71	1.21	2.10	0.82	5019	751	735	0.15
$x=0.25$	1.65	0.57	0.89	1.98	0.83	4787	1379	1280	0.27
$x=0.5$	1.60	0.42	0.95	1.86	0.86	4642	1713	1528	0.33
$x=0.75$	1.40	0.31	0.70	1.51	0.93	4062	1856	1577	0.39
$x=0.833$	1.28	0.34	0.80	1.33	0.96	3714	1183	1082	0.29
$x=0.875$	1.14	0.33	0.81	1.23	0.92	3307	1088	991	0.30
$x=0.916$	1.11	0.36	0.75	1.17	0.94	3220	895	835	0.26
$x=1$	0.84	0.51	0.85	1.01	0.82	2437	659	617	0.25

change slightly for different nitrogen vacancy arrangements (not shown here). In fact, in a localized system, such as transition metal oxides, the vacancy may change the distance between the magnetic atoms, or cut off the interaction mediate of magnetic atoms. But in an itinerant system, the vacancy influences magnetism mainly by changing the number of itinerant electrons. When the vacancy distance is a, around the vacancy, there are two Mn1 and four Mn2 of the total 24 Mn atoms. For the other two cases, there are zero Mn1 and six Mn2 of the total 24 Mn atoms. Such small difference could not lead a large variation for the number of itinerant electrons. In the real sample with good quality, the vacancies are randomly distributed. The vacancy arrangements must be a combination of the mentioned three cases. Therefore, our calculation can qualitatively describe the electronic property of real sample.

Thus, we figure out the role of nitrogen for magnetism: (a) With nitrogen concentration decreasing, the spin-down states move towards the higher energy remarkably, which enhances the exchange splitting energy ΔE_{ex}; (b) The loss of nitrogen reduces the Mn-N hybridization, which makes the 3d electrons of Mn tend to occupy the spin-up state. According to the Stoner criterion, a larger value of $N(E_F)$ (non-magnetic state) makes electrons more polarized. In our case, the nitrogen deficiency enhances the $N(E_F)$ (non-magnetic state), which is due to the reduced Mn-N hybridization and the resulting narrowing of the Mn-d bands. Therefore, the nitrogen deficiency enhances the spin polarization. Sieberer *et al.*[16] reported a similar case for AlC_xNi_3 and GaC_xNi_3.

In our previous experimental work, the AlN_xMn_3 samples show very high T_c up to 818 K, and it seems the nitrogen deficiency enhances T_C. Here, we estimated the T_C of AlN_xMn_3 ($x = 0$, 0.25, 0.5, 0.75, and 1) using the widely used model derived by Mohn and Wohlfarth[27]

$$\frac{T_C^2}{T_S^2} + \frac{T_C}{T_{SF}} - 1 = 0, \tag{1}$$

where T_S is Stoner temperature derived from Stoner model of itinerant electron magnetism, which can be approximately estimated using the relation[28,31]

$$T_S = \frac{\Delta E_{ex}}{4k_B}. \tag{2}$$

And the spin fluctuation temperature T_{SF} is given by[27]

$$T_{SF} = \frac{m^2}{10k_B\chi_0}, \tag{3}$$

where the exchange enhanced susceptibility χ_0 derived by Wohlfarth[29] and Gersdorf[30] can be expressed as

$$\chi_0^{-1} = \frac{1}{2\mu_B^2}\left[\frac{1}{2N_{\mathrm{Mn}}^{\uparrow}(E_F)} + \frac{1}{2N_{\mathrm{Mn}}^{\downarrow}(E_F)} - I\right], \tag{4}$$

where m is the magnetic moment of a Mn atom, and I is the Stoner exchange integer given by $\Delta E_{ex} = Im$.[32] Our calculated parameters and critical temperatures are listed in Table I.

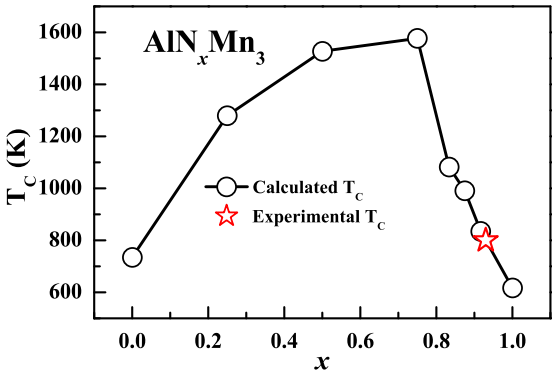

FIG. 6. The theoretically estimated and experimental T_C of AlN_xMn_3.

As expected, $T_S \gg T_C$, since the Stoner excitations (also called single-particle excitation) are thought to destroy magnetic order scale with T_F (Fermi temperature) and are thus too much weak at normal temperature to create any sizable effect.[32] All the ratios $T_C/T_S < 0.5$ suggest the AlN_xMn_3 belong to the spin fluctuation system.[27] Therefore, T_C can be scaled by T_{SF}, which is directly determined by m, $N_{\mathrm{Mn}}^{\uparrow}(E_F)$, and $N_{\mathrm{Mn}}^{\downarrow}(E_F)$ listed in Table I. As mentioned above, the variety of m is due to the influence of nitrogen concentration. The changes of $N_{\mathrm{Mn}}^{\uparrow}(E_F)$ and $N_{\mathrm{Mn}}^{\downarrow}(E_F)$ can be attributed to the variation of the ΔE_{ex} and location of E_F, which originate from the influence of nitrogen, too. As the nitrogen concentration is close to 1, the nitrogen deficiency enhances the T_C, which is coincident with our previous experimental results. The maximum T_C is established as $x = 0.75$, and with further reducing the nitrogen concentration, the calculated T_C decreases.

The predicted T_C is shown in Fig. 6. The estimated T_C for the ideal $AlNMn_3$ is 617 K. The measured T_C of our previously synthesized nitrogen-deficient samples are 818, 802, and 774 K, which are close to the estimated T_C of AlN_xMn_3 for $x = 0.916$ with the value of 835 K. Thus, the real concentration of nitrogen for our previously synthesized AlN_xMn_3 can be estimated between $x = 0.92$ and $x = 0.95$. The experimental lattice variety of the synthesized samples is only about 0.17%, which is consistent with such small nitrogen concentration difference. Clearly, the magnetic property of AlN_xMn_3 is very sensitive to the nitrogen concentration.

IV. CONCLUSION

In conclusion, we performed a theoretical investigation on antiperovskite nitrides AlN_xMn_3 through the first-principles calculation based on DFT theory. Different magnetic states were tested, and it turns out that AlN_xMn_3 ($x = 1$ to $x = 0$) show FM ground states. The total magnetic moments in a cell increases with the decreasing of nitrogen concentration. Based on the calculated band structure and DOS, the role of nitrogen for magnetism is figured out. The nitrogen deficiency reduces the Mn-N hybridization, which narrows Mn-d bands and enhances the spin polarization. Using Mohn and Wohlfarth's model,[27] we estimated T_C for AlN_xMn_3. Our results suggest the magnetism of AlN_xMn_3 can be described by spin fluctuation theory. By comparing the theoretically estimated and experimental value of T_C, we evaluated the real concentration of the nitrogen for the

sample synthesized previously. Evidently, nitrogen plays a very important role on the magnetic properties of the manganese nitride antiperovskites AlN_xMn_3.

ACKNOWLEDGMENTS

This work was supported by the National Key Basic Research under Contract No. 2011CBA00111, and the National Nature Science Foundation of China under Contract Nos. 91222109, 11274311, 51171177, 11174295, U1232139, and 50701042. The calculations were partially performed at the Center for Computational Science, CASHIPS.

[1]T. He, Q. Huang, A. P. Ramirez, Y. Wang, K. A. Regan, N. Rogado, M. A. Hayward, M. K. Haas, J. S. Slusky, K. Inumara, H. W. Zandbergen, N. P. Ong, and R. J. Cava, Nature **411**, 54 (2001).
[2]M. Uehara, T. Yamazaki, T. Kôri, T. Kashida, Y. Kimishima, and I. Hase, J. Phys. Soc. Jpn. **76**, 034714 (2007).
[3]K. Kamishima, T. Goto, H. Nakagawa, N. Miura, M. Ohashi, N. Mori, T. Sasaki, and T. Kanomata, Phys. Rev. B **63**, 024426 (2000).
[4]Y. B. Li, W. F. Li, W. J. Feng, Y. Q. Zhang, and Z. D. Zhang, Phys. Rev. B **72**, 024411 (2005).
[5]T. Tohei, H. Wada, and T. Kanomata, J. Appl. Phys. **94**, 1800 (2003).
[6]M. H. Yu, L. H. Lewis, and A. R. Moodenbaugh, J. Appl. Phys. **93**, 10128 (2003).
[7]K. Takenaka and H. Takagi, Appl. Phys. Lett. **87**, 261902 (2005).
[8]K. Takenaka, K. Asano, M. Misawa, and H. Takagi, Appl. Phys. Lett. **92**, 011927 (2008).
[9]K. Asano, K. Koyama, and K. Takenaka, Appl. Phys. Lett. **92**, 161909 (2008).
[10]E. O. Chi, W. S. Kim, and N. H. Hur, Solid State Commun. **120**, 307 (2001).
[11]J. C. Lin, B. S. Wang, P. Tong, S. Lin, W. J. Lu, X. B. Zhu, Z. R. Yang, W. H. Song, J. M. Dai, and Y. P. Sun, Scr. Mater. **65**, 452–455 (2011).
[12]M.-h. Yu, L. H. Lewis, and A. R. Moodenbaugh, J. Magn. Magn. Mater. **299**, 317 (2006).
[13]K. Takenaka, T. Shibayama, K. Asano, and K. Koyama, J. Phys. Soc. Jpn. **79**, 073706 (2010).
[14]P. Tong, Y. P. Sun, B. C. Zhao, X. B. Zhu, and W. H. Song, Solid State Commun. **138**, 64 (2006).
[15]L. H. Lewis, D. Yoder, A. R. Moodenbaugh, D. A. Fischer, and M.-H. Yu, J. Phys.: Condens. Matter **18**, 1677 (2006).
[16]M. Sieberer, P. Mohn, and J. Redinger, Phys. Rev. B **75**, 024431 (2007).
[17]J. C. Lin, B. S. Wang, P. Tong, W. J. Lu, L. Zhang, X. B. Zhu, Z. R. Yang, W. H. Song, J. M. Dai, and Y. P. Sun, Appl. Phys. Lett. **98**, 092507 (2011).
[18]Y. Ouyang, H. Chen, M. Tong, Y. Du, Y. Feng, and X. Zhong, Comput. Mater. Sci. **44**, 97 (2008).
[19]W. J. Takei, R. R. Heikes, and G. Shirane, Phys. Rev. **125**, 1893 (1962).
[20]C. L. Li, Y. Yang, L. Y. Lv, H. B. Huang, Z. H. Wang, and S. G. Yang, J. Alloys Compd. **457**, 57 (2008).
[21]X. Gonze, B. Amadon, and E. A. Anglade, Comput. Phys. Commun. **180**, 2582 (2009).
[22]X. Gonze, J. M. Beuken, R. Caracas, F. Detraux, M. Fuchs, G.-M. Rignanese, L. Sindic, M. Verstraete, G. Zerah, F. Jollet, M. Torrent, A. Roy, M. Mikami, P. Ghosez, J.-Y. Raty, and D. Allan, Comput. Mater. Sci. **25**, 478 (2002).
[23]X. Gonze, Z. Kristallogr. **220**, 558 (2005).
[24]J. P. Perdew, K. Burke, and M. Ernzerhof, Phys. Rev. Lett. **77**, 3865 (1996).
[25]C. Hartwigsen, S. Goedecker, and J. Hutter, Phys. Rev. B **58**, 3641 (1998).
[26]H. J. Monkhorst and J. D. Pack, Phys. Rev. B **13**, 5188 (1976).
[27]P. Mohn and E. P. Wohlfarth, J. Phys. F: Met. Phys. **17**, 2421 (1987).
[28]Q. Qi, R. Skomski, and J. M. Coey, J. Phys.: Condens. Matter **6**, 3245 (1994).
[29]E. P. Wohlfarth, Phys. Lett. **3**, 17 (1962).
[30]R. Gersdorf, J. Phys. Radium **23**, 726 (1962).
[31]H. Ibach and H. Lüth, *Solid State Physics* (Springer, Berlin, 1993).
[32]P. Mohn, *Magnetism in the Solid State: An Introduction* (Springer, Berlin, 2006).